ISSN 1067-8212, Russian Journal of Non-Ferrous Metals, 2018, Vol. 59, No. 1, pp. 93–101. © Allerton Press, Inc., 2018.

PHYSICAL METALLURGY AND HEAT TREATMENT

Microstructural and Mechanical Characterization of as Weld and Aged Conditions of AA2219 Aluminium Alloy by Gas Tungsten Arc Welding Process[1]

S. Arunkumar[a], P. Sathiya[a, *], K. Devakumaran[b], and S. Ramesh Kumar[c]

[a] *Department of Production Engineering, National Institute of Technology Tiruchirappalli, Tamilnadu, 620015 India*

[b] *Welding Research Institute, BHEL, Tiruchirappalli, Tamilnadu, 620015 India*

[c] *School of Mechanical Engineering, SASTRA University, Thanjavur, Tamilnadu, 620015 India*

**e-mail: psathiya@nitt.edu*

Received April 3, 2017

Abstract—In this article, Welding of AA2219 aluminium alloy using Gas tungsten arc welding process (GTAW) and evaluation of metallurgical, mechanical and corrosion properties of the joints are discussed. The weld samples were subjected to ageing process at the temperature range of 195°C for a period of 5 h to improve the properties. AA2219 aluminium plates of thickness of 25 mm were welded using gas tungsten arc welding (GTAW) process in double V butt joint configuration. The input parameters considered in this work are welding current, voltage and welding speed. Tensile strength and hardness were measured as performance characteristics. The variation in the properties were justified with the help of microstructures. The same procedures were repeated for post weld heat treated samples and a comparison was made between as weld condition and age treated conditions. The post weld heat samples had better tensile strength and hardness values on comparing with the as weld samples. Fracture surface obtained from the tensile tested specimen revealed ductile mode of failure.

Keywords: AA2219 aluminum alloy, GTAW, ageing, microstructure, tensile property, hardness, fractography

DOI: 10.3103/S1067821218010030

1. INTRODUCTION

AA2219 alloy is an Al–Cu–Mn ternary alloy with good cryogenic properties (temperatures in the range of 200 to –200°C) [1] and it comes under the category of nonferrous material. AA2219 has excellent weldability and very specific strength. AA2219 has other advantages like good high ductility, formability and also reasonable corrosion resistance. Electron beam welding (EBW) and friction stir welding (FSW) are found to be the best welding processes for obtaining high strength welds. But, on comparing with the GTAW process, EBM and FSW processes are not economical. For all grades of aluminium alloys, GTAW is considered as the most ecomical and suitable process in producing good quality weld joints [2]. However, based on the current literatures the authors have identified few limitations in fusion welding of aluminum alloys. Solidification cracking and reduction in weld metal strength are one of the major issues in joining aluminium alloys. The major problems in the welding of aluminium alloys are mainly contributed by the varying percentage of alloying elements present in the alloys. If the percentage of alloying elements are very low level, then the volume of liquid films present at the grain boundaries are also very little which in turn reduces the crack formation. If the percentage of alloying elements present in the alloy are very high as in AA2219 alloy which has 6.33% copper, it leads to excess availability of liquid in solidification that flows in to the cracks and helps in healing the cracks. In general, most of the works related to joining of AA2219 shows a 40% drop in tensile strength on comparing with the base metal. The above mentioned phenomenon is seen in both autogenous welds as well as in heterogenous welds. Tensile strength reduction in the welds were mainly because of melting and quick resolidification which helps to dissolve strengthening precipitates and becomes as a solution treated material. Precipitation solidified AA2219 aluminum composite is used as a part of the welded cryogenic fuel tank on account of its outstanding mechanical properties over a wide temperature from –250°C to 250°C [1]. Due to its excellent weldability, AA2219 is best suitable in aerospace industry. The excess amount of copper present in the alloy helps in avoiding hot crack formation [3]. Gas tungsten arc welding (GTAW) carried out with zirconium and scandium as filler material helped in improving the corrosion properties of the AA2219

[1] The article is published in the original.

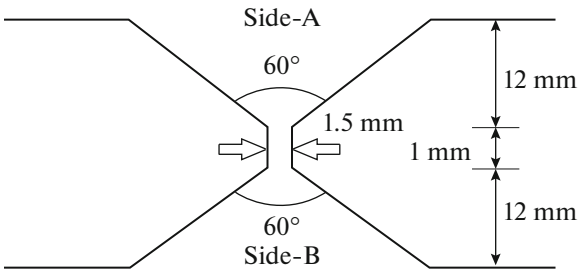

Fig. 1. Schematic diagram showing locations side-A and side-B of double V groove.

weld joints. In addition to that, presence of Sc and Zr to the weld zone during welding helped in refining the grains and improving the mechanical properties [4].

The AA2219 alloy joints were made using different welding processes namely, gas tungsten arc welding, electron beam welding and friction stir welding and it was observed that comparatively friction stir welded AA2219 had better properties than the joints made with EBM and GTAW [5]. Zigzag line effect on the quality of friction stir welded AA2219-O alloy was studied and it was observed that zigzag line had no influence on the weld properties [6]. In friction welding of AA2219-T6, it was observed that with increase in welding speed, tensile properties and joint efficiency also got increased significantly [7]. Friction stir welding was used for joining AA2219-T87 alloy and weldments microstructure, mechanical properties, corrosion resistance were studied and it was understood that the dissolution and strengthening precipitates coarsening in the weld resulted in weld region softening [8]. Advanced techniques are been developed to rise cooling rates in GTAW process and it helped in improving the tensile strength and hardness of the GTAW welded Aluminium alloys [9]. AA2219 aluminium alloy joints by variable polarity tungsten inert gas (VPTIG) welding process and the effects of post weld heat treatment (PWHT) on the tensile properties, microstructure and fatigue behaviour of the welded joints were investigated. The experimental results showed that, compared with the AW samples, the microstructure characteristics and mechanical properties of the AA2219 joints after PWHT were significantly improved. The improvement of yield strength, ultimate tensile strength, and fatigue strength are 42.6, 43.1, and 18.4%, respectively [10].

Based on the literature survey, it was understood that the authors have so far focused on joining AA2219 alloys with different heat inputs. Considerable amount of works were carried out in friction stir welding of AA2219 alloys. From the literatures, it is also understood that only few works were done in heat treatment of AA2219 weldments. Hence In this work, an attempt is made to join AA2219 alloys using GTAW process followed by ageing of the welded samples. An comparison is made between the welded AA2219 alloy and aged weld specimens with respect to tensile strength and hardness.

2. EXPERIMENTAL PROCEDURE

AA2219 plates with 25 mm thick were joined in butt configuration by GTAW process. The plates were rigidly fine-tuned to avoid distortion during welding. Figure 1 shows the double V groove design along with the set of shielding gas setup. The electrodes and base plates were acid pickled, washed in water and acetone followed by wire brushing prior to welding. The welding parameters were choosen based on the results obtained from the non traditional optimization techniques and the same welding parameters are presented in the Table 1. The automatic mode of welding process includes the input parameters as arc voltage and welding current, which were quantified utilizing a digital meter fitted in the welding power source. In the double V-groove, initially, welding was carried out on side-B followed by side-A (Fig. 1).

Base metal and filler wire chemical compositions are shown in Table 2.

Solutionizing and ageing heat treatments were performed for butt joined AA2219 alloys. Solutionizing were performed for butt welded specimen at a temperature of 545°C up to 1 h, followed by rapid quenching into warm water. Soon after quenching, the samples were treated with aged conditions at a temperature of 195°C up to 5 h. The quality of the welds were assessed with hardness, tensile properites. Required

Table 1. Welding parameters

Welding current, A	125
Arc voltage, V	8
Welding speed, cm min^{-1}	10
Heat input, kJ cm^{-1}	6
Filler wire diameter and specifications	1.5–2.5 mm & ER 2319
Shielding gas	Commercially pure argon at gas flow rate of 15 lpm
Polarity	AC
Tungsten electrode size and type	3.15 mm diameter and 2% Zirconated

Table 2. Base metal and filler wire Chemical Compositions (mass fraction, %)

	Cu	Mn	Fe	Zr	V	Si	Ti	Zn	Al
Base metal	6.33	0.34	0.13	0.12	0.07	0.06	0.04	0.02	Bal.
Filler wire (ER 2319)	6.21	0.39	0.18	0.11	0.09	0.09	0.10	–	Bal.

Schematic diagram of GTAW process is shown in Fig. 2.

size of the specimens were cut, polished, etched with the Kellers reagent containing 95 mL water + 2.5 mL HNO_3 +1.5 mL HCI +1.0 mL HF to expose the microstructure variation. Weldment microstruture was taken with the help of optical microscope and scaning electron microscope. In accordance with the ASTM E8 Standards the tensile test specimens were prepared for both as weld and age treated weld samples using electrical discharge machine and tensile test was then conducted using a 40 t universal testing machine at room temperature. Yield, tensile strength and elongation percentage were measured. The fractography of tensile samples were analysed with the help of Scanning electron microscope (JEOL 5610 LV) to study the fracture surface. Before SEM fractrography, the fracture surfaces were cleaned with acetone and carbon tetrachloride (CCl_4). Three samples were tested at each condition and their average values were recorded.

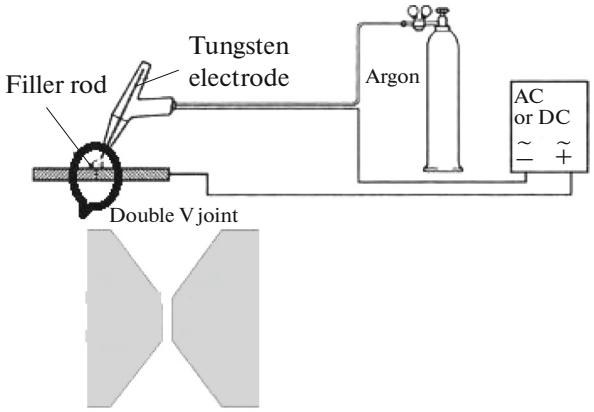

Fig. 2. Schematic diagram of GTAW process.

3. RESULTS AND DISCUSSION

3.1. Microstructure of the Welded Joints

Base material optical and SEM microstructures were presented in Figs. 3a, 3b. From Fig. 3a it is noted that the grains are coarser and elongated with panacke shaped grain boundaries along with some of the dark particles in the form of precipitates and further it was confirmed through SEM microstructure (Fig. 3b). The line intercept method was used to measure the grain size. The grain sizes in the as received base material were from 50 to 65 μm.

Metallographical studies was performed on the weldments to examine the microstructural changes that occurred within the material as well as in the areas weld joint and also at aged treated condition From Fig. 4a, refined grains were studied along with the dendritic spacing were found to be some what in smaller size. From Fig. 4a, it was clear that the optical microstructure in the weld metal were unable to showcase any kind of strengthening precipitates which contained α-Al grains and comparatively high portion of

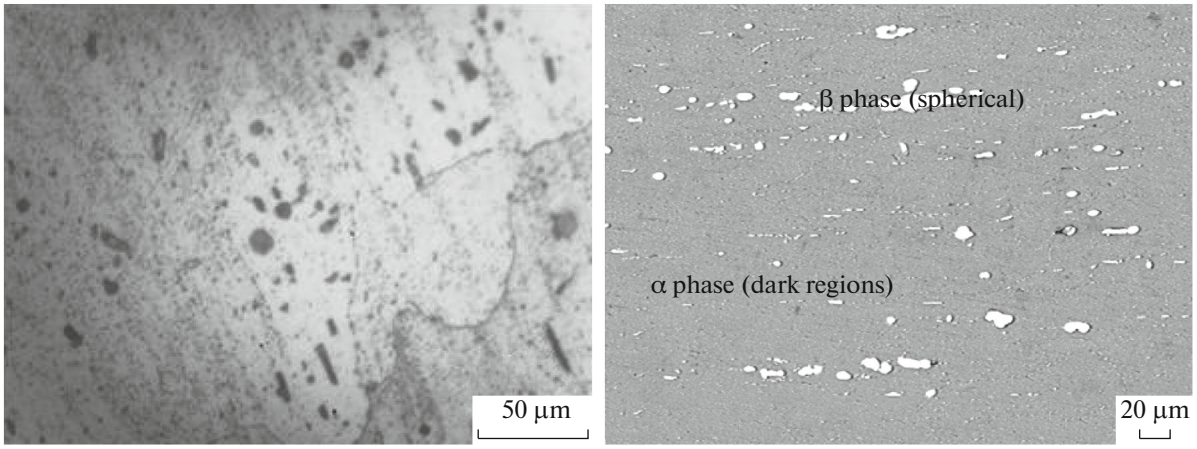

(a) Optical microstructure (b) SEM microstructure

Fig. 3. Base metal microstructures.

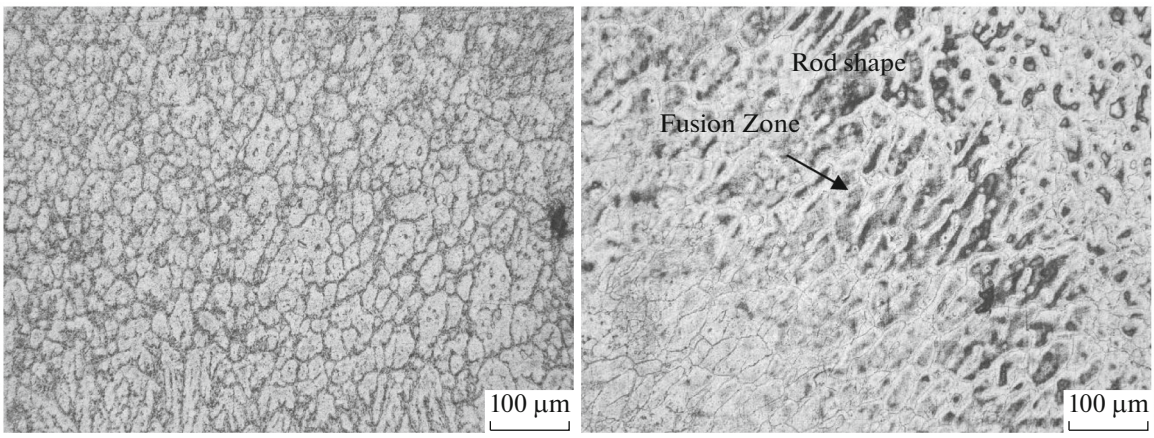

(a) As weld joint (b) Fusion line

Fig. 4. As welded microstructure of AA2219 weld joint.

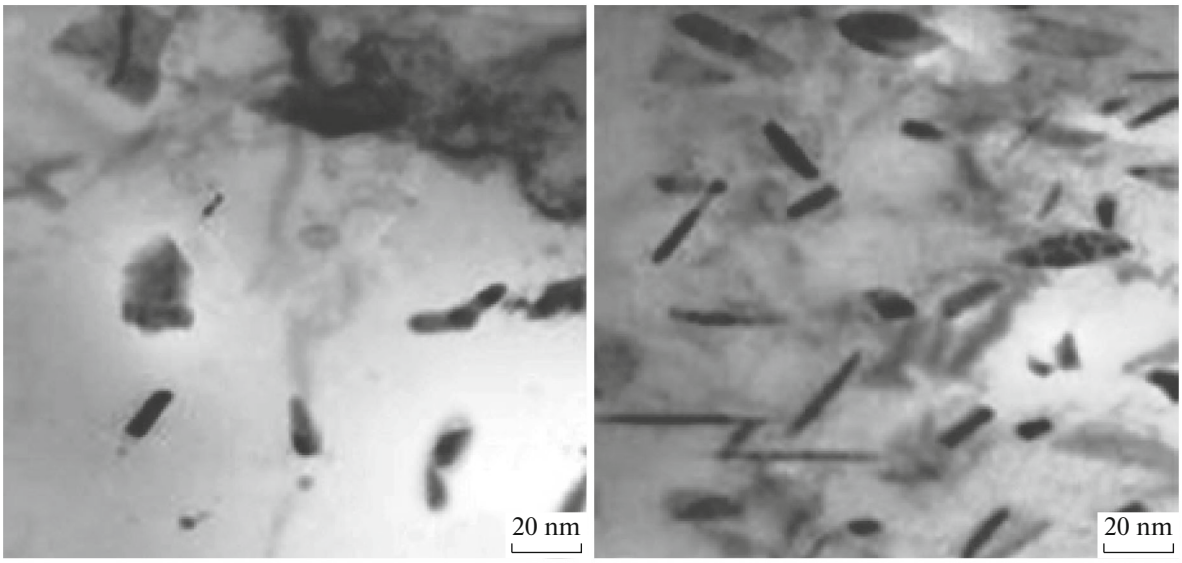

(a) As weld joint (b) Age treated weld metal

Fig. 5. TEM micrographs.

intermetallic phases distributed at the aluminium dendrite boundaries. It can be seen that the Al_2Cu stage is totally dissoloved in the α-Al strong arrangement except for little particles which couldn't be broken up even after prolonged solution in zing time [11]. The variation of grain size and precipitates is regarded as the main cause of softening in both FZ and HAZ [12]. The amount of dendrites present is negligible compared to the distribution of grains in the weld zone. Similar kind of dendrite structure were observed in weld and base metal. Fusion zone is clearly seen in Fig. 4b.

In order to find the presence of precipitates in the weld metal a further investigation is carried out by transmission electron microscope (TEM). TEM structure for both ss weld and age treated weld structures are shown in Figs. 5a, 5b.

Figure 5a shows that most of the precipitates are fully dissolved in the matrix and few precipitates are clearly visible. From Fig. 5b shows clearly that the that age treated weld had more precipitates than as welded joint. The needle shaped $CuAl_2$ precipitates were distributed homogeneously inside the grain. These precipitates enhanced the strength aspects of AA2219 alloy. The confirmation of these precipitates were analysed through EDX. Due to high temperature and for a long period of time, Cu were diffused out of solution and in large precipitate regions. Due to ageing, the increased regions of $CuAl_2$ precipitates were grown together. The age treated weld microstructures are shown in Fig. 6.

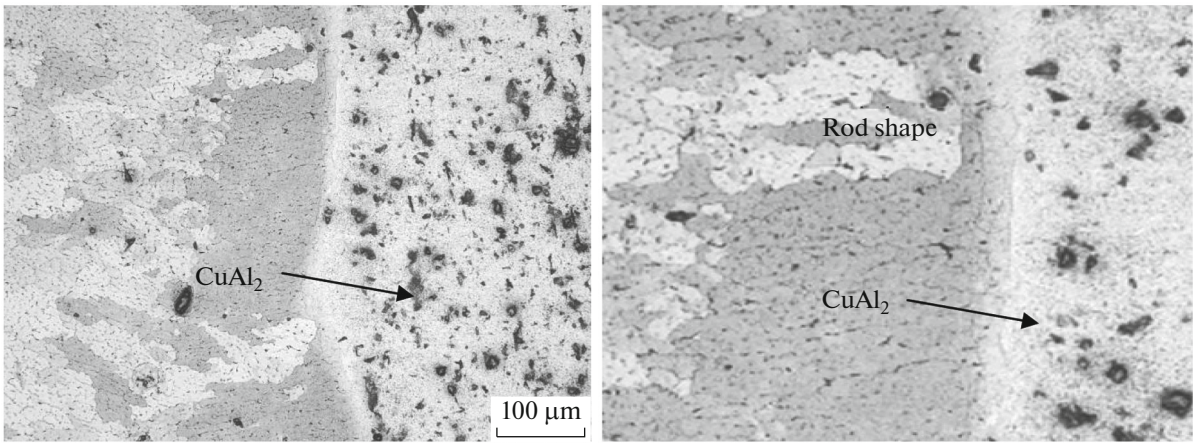

Fig. 6. Aged microstructure of AA2219 weld joint.

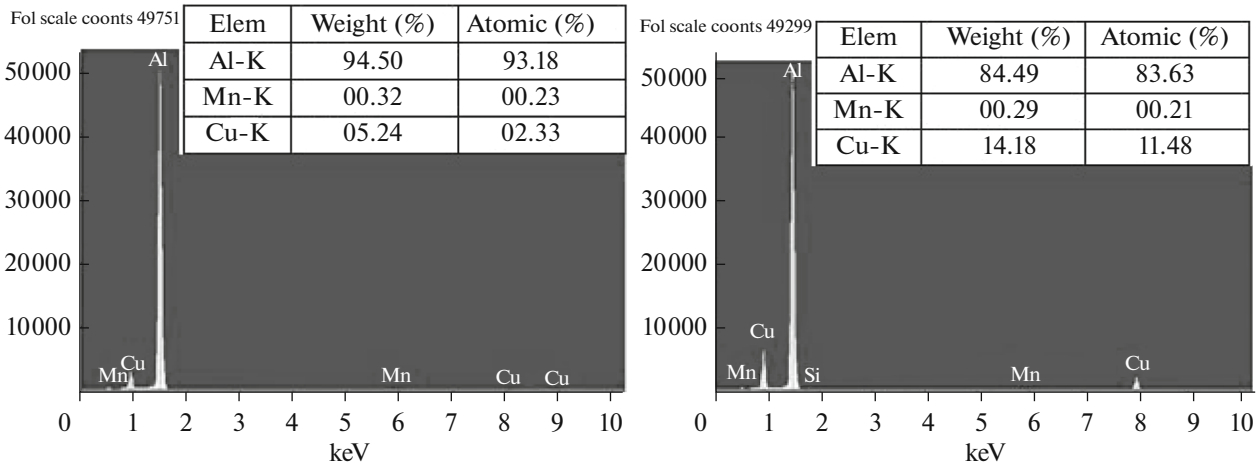

(a) As weld joint (b) Age treated weld metal

Fig. 7. EDAX results.

Figure 6 shows that age treated microstructure contains high amount of dendrite structure when compared to as weld region. The size of the dendrite presents in the age treated weld region was almost similar to the needle (or) rod like structure. The orientation of all the dendrites was at most in the same direction towards the heat affected zone. The distribution of dendrites as well as their size in the age treated region has higher spatial distribution. Electron Dispersive Analysis was done on the weld microstructure to reveal the elements of precipitates. Figure 7 shows the outcomes of EDAX. It reveals that all the peaks observed in the EDAX analysis are Al–Cu based precipitates.

From Fig. 7a it can be seen that weld contained 5.24% copper and 94.5% aluminum. The precipitates of age treated weld joints contained greater fraction of copper than the as welded joint which is apparent from the EDAX results presented in Fig. 7b. The variations of chemical composition obtained in the welds showed the presence of higher amount of precipitates in the age treated weld joint (Fig. 5b).

3.2. Hardness of the as Weld and Age Treated Welded Joints

The hardness measurements were measured along the transverse direction of the joints to correlate with the microstructural evaluation. Microhardnes measurements were measured at equal intervals of 0.5 mm starting from weld centre. The microhardness values for different zones are shown in Fig. 8.

From Fig. 8 it is observed that the microhardness measurement, weld region hardness values were lesser than base metal. The prime reason for the failure taking place in the weld region is due to reduction value of the hardness values of weld and age treated. The key part in determining the hardness and tensile properties of the weld region of AA2219 alloys is played by size and distribution of $CuAl_2$ [13]. During GTA welding, due to the slow cooling rate all the precipitates were not dissolved in the weld zone and only a few precipitates got dissolved and a few precipitates were retained in the weld region throughout the matrix (Fig. 5a).

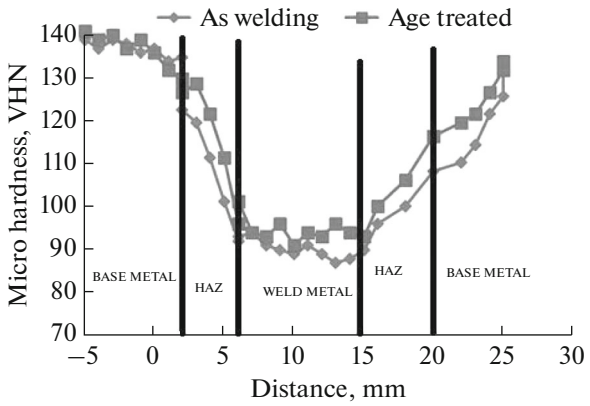

Fig. 8. Microhardness profiles for different zones.

Size and distribution of the precipitates might control the weld metal properties. Under the as-welded conditions, the mechanism of solid solution strengthening were involved as primary mechanisms. But distribution of particles caused strain localization under age-treated conditions [14]. The improvement of hardness property is not only due to the size and distribution of precipitates, but also due to the composition of precipitates [15]. The copper content based precipitates which gave better resistant to indentation is also the reason for higher hardness in the age treated weld joints. Hence, it is confirmed from Fig. 5b that a high amount of $CuAl_2$ needle shaped precipitates were present in the weld region.

3.3. Tensile Properties of the Joints

Three samples were prepared and verified experimentally to measure tensile properties as weld and aged treated weld and shown in Table 3. The average values were calculated and presented in the Table 3. Base metal tensile strength is shown for comparison. The main reason for improved tensile strength of the material are fine $CuAl_2$ precipitates. These strengthening precipitates get formed because of solution treatment followed by subsequent artificial ageing process. Majority of the precipitates belong to Cu and Al based precipitates [16]. Based on the tensile test values we confirmed that the failure had occurred in the weld region. From Table 3 it is seen that the tensile strength showed a drastic reduction of the as weld and age treated joint strength as compared with the base metal [16]. This happened due to minor variation in the work hardening behaviour which may be due to lower dynamic recovery. The yield strength (YS) and tensile strength (TS) of the base metal were 390 and 470 MPa respectively. The YS and TS of as weld joint strengths were 201 and 280 MPa respectively i.e., indicating 44% reduction for YS and 40% reduction for TS. The formation of finer grains caused by pulsed current is the also one of the reason for enhanced tensile and hardness properties of the joints [17]. This reduction in strength was because of strengthening precipitates dissolution in the weld zone and the presence of larger columner dendrite grain structures [18, 19]. Comparatively, the age treated tensile strengths showed higher YS and tensile strength of 265 MPa and 337 MPa. This suggested that there is an improvement in tensile strength of age treated weld by 24% for YS and 17% for TS respectively. Weld joint efficiency (ratio between strength of weld metal and strength of base metal) under different conditions of AA2219 weld joints have been also given in Table 3. Due to the ageing treatment, the weld joint efficiency was improved around from 60 to 70%. The presence of $CuAl_2$ and grain refinement has a distinct influence in improving the tensile strength of age treated weld joints. The distribution of grains was in heterogeneous manner in case of as welded joint but in the case of aged treated joints the distribution of grains found to be homogeneous distribution [20]. In addition to that, due to orientation of the grains and distribution of the grains in aged treated joints hardness and tensile got increased more than the as weld joint.

At this juncture, it was inferred that, in general, AA2219 weld joint exhibits only 50% of weld joint efficiency by using conventional arc welding processes. In the literature, it was reported that, long term ageing will improve the weld joint efficiency. Based on the literature, 195°C ageing temperature and 5 h chocking time was chosen. Due to this ageing treatment conditions and pusing effect in GTAW process, the joint efficiency of AA2219 weld joint was improved around from 60 to 70%. However, the effect of different ageing conditions on properties of AA2219 weld joints shall be studied further in details. This is not in the scope of present work.

Table 3. Tensile properties of as welded and age treated joints

Materials	Yield strength, MPa	Tensile strength, MPa	% of Elongation
As welded conditions			
Base Metal	360	470	14.8
As welded	201	280	10.1
Joint efficiency	—	59.5%	—
Age treated conditions			
Base metal	360	470	14.8
Aged Conditions	265	337	12.0
Joijnt efficiency	—	71.7%	—

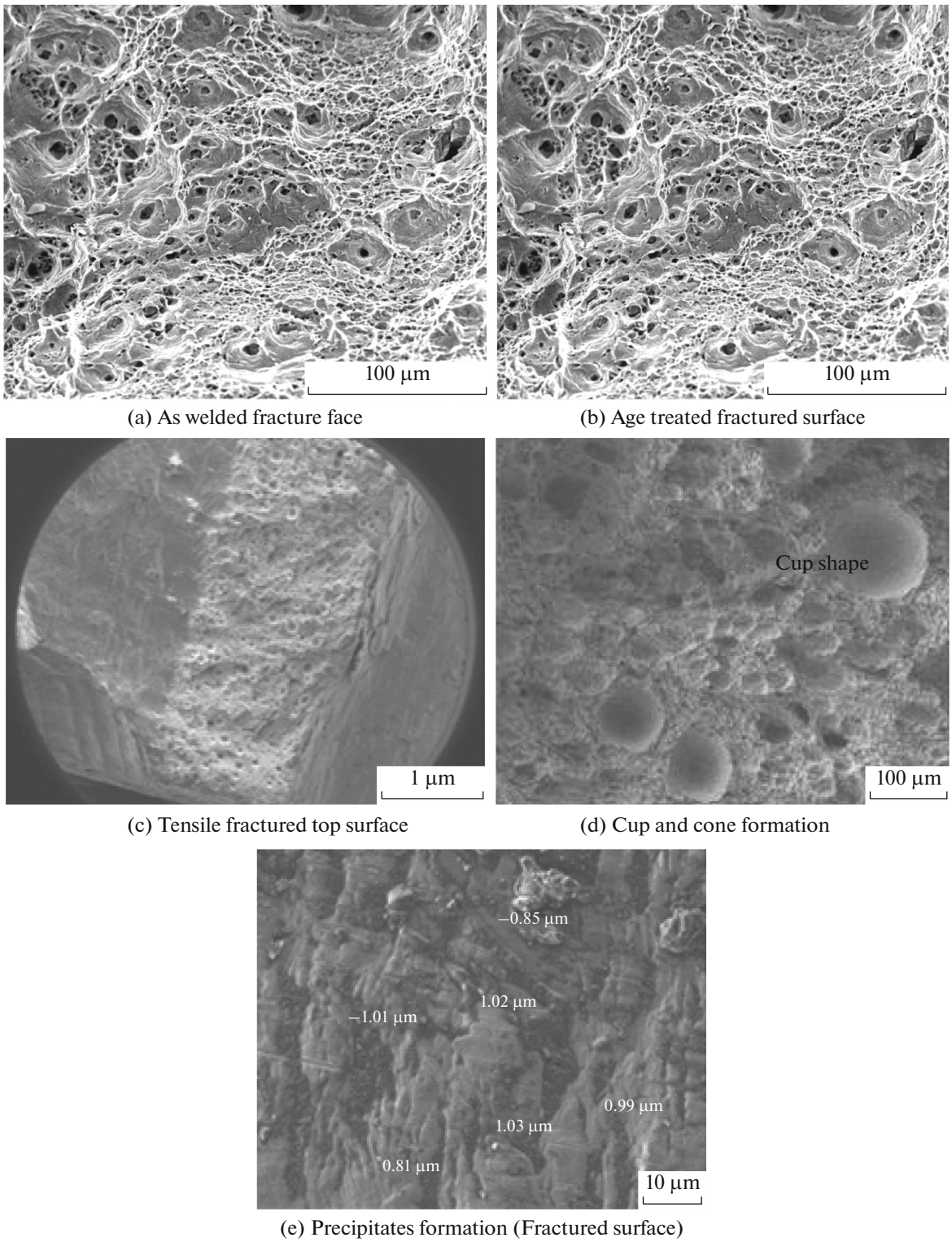

(a) As welded fracture face (b) Age treated fractured surface

(c) Tensile fractured top surface (d) Cup and cone formation

(e) Precipitates formation (Fractured surface)

Fig. 9. SEM fractographs of as weld and age treated tensile fractured samples.

3.3.1. Fractogrphy of the tensile fractured surfaces. Fractography of the welded condition and age treated condition are shown in Figs. 9a–9e.

Figures 9a, 9b shows that as welded and age treated tensile fracture morphology exhibited predominantly ductile mode of failure. Finer dimples sizes and as well

as smaller micro voids were seen in the fractured surfaces of the both tensile tested specimens. Particularly, age treated tensile samples dimples size were very finer than the weld conditions. Due to very fine dimple size, the tensile values are higher than the as welded tensile results. Comparatively base metal had better hardness than as weld and age treated condtions welds. Hence, it is found that the elongation in tensile test would be narrowed primarily to the weld and the remaining portion of the tensile sample was not deformed significantly [21, 22].

On further welded condition the cup and cone shape fracture occurred and it is clearly observed in the Figs. 8c, 8d. On measuring very small dendrites were observed it was around 0.23 to 0.25 μm. But in the case of heat treated condition, the dendrite size was around 0.1–0.15 μm (Fig. 9e). In this condition, the dendrites will improve the strength and the precipitate facilitates an important role in achieving the higher strength [23]. Higher ductility is encountered in the middle portion than the side portions.

4. CONCLUSIONS

AA2219 aluminium alloy butt weld was performed by Gas Tungsten Arc Welding process (GTAW). GTAW weld samples were further studied on age treated conditions. Tensile properties and tests were performed. Microstrucure characterization and tensile fractured surface analysis were evaluated for the as welded and age treated conditions of AA2219 butt welded sample. Based on this study, the following conclusions are drawn.

• As weld and aged weld had dendritic grains and the size of the aged weld was comparatively finer than the as weld grain size. In weld, the precipitates were completely dissolved, whereas in the aged condition of the weld, the precipitates were large in number and was clearly seen in TEM. The needle like shapes is due to the presence of $CuAl_2$ precipitates.

• Weld hardness is controlled due to the $CuAl_2$ precipitates seen in the weld controlled by the composition to a greater extent. Comparatively base metal had higher hardness and the hardness of the weld increased after ageing process.

• Tensile strength of base metal was better than the weld and aged condition tensile strength. The reduction in the tensile strength was attributed to the increased columnar dendrites size and presence of $CuAl_2$ precipitates. The improvement in tensile strength after ageing might be attributed to the refinement of the dendritic shaped grains.

• Fractography of the tensile tested weld and aged samples revealed the presence of dimples which in turn confirmed the ductile mode of failure. Comparatively the dimple size in the aged condition of weld was finer which in turn helped in increasing the strength after ageing process.

ACKNOWLEDGMENT

We acknowledge Shri. P. Sankaravelayuthan, Dy. General Manager, MMD/MME, VSSC, ISRO, Thiruvanandapuram-695022 to provide the base material and WRI, BHEL, Trichy, Tamilnadu to carry out the welding trials.

REFERENCES

1. Banhart, J., Chang, C.S.T., Liang, Z., Wanderka, N., Lay, M.D.H., and Hill, A.J., *Adv. Eng. Mater.*, 2010, vol. 12, pp. 559–571.
2. Tosto, S., Nenci, F., and Hu, J., Microstructure and properties of electron beam welded and post welded 2219 aluminium alloy, *Mater. Sci. Technol.*, 1996, vol. 12, no. 4, pp. 323–328.
3. Koreswara Rao, S.R., Madhusudhan Reddy, G., Srinivasa Rao, K., Srinivasa Rao, P., Kamaraj, M., and Prasad, Rao, K., Gas tungsten arc welded AA2219 alloy using scandium containing fillers-mechanical and corrosion behavior, *Trans. Ind. Inst. Met.*, 2004, vol. 57, no. 5, pp. 451–459.
4. Seshagiri, P.C., Nair, B.S., Reddy, G.M., Rao, K.S., Bhattacharya, S.S., and Rao, K.P., Improvement of mechanical properties of aluminium–copper alloy (AA22219) GTA welds by Sc addition, *Sci. Technol. Weld. Join.,* 2008, vol. 13, no. 2, pp. 146–158.
5. Malarvizhi, S. and Balasubramanian, V., Effect of welding processes on AA2219 aluminum alloy joint properties, *Trans. Nonfer. Met. Soc. China*, 2011, vol. 21, pp. 962–973.
6. Liu, H.J., Chen, Y.C., and Feng, J.C., Effect of zigzag line on the mechanical properties of friction stir welded joints of an Al–Cu alloy, *Scripta Mater.*, 2006, vol. 55, no. 3, pp. 231–234.
7. Weifeng, Xu., Liu, J., Luan, G., and Don, C., Microstructure and mechanical properties of friction stir welded joints in 2219–T6 aluminum alloy, *Mater. Des.*, 2009, vol. 30, no. 9, pp. 3460–3767.
8. Bala Srinivasan, P., Arora, K.S., Dietzel, W., Pandy, S., and Schaper, M., Characterization of microstructure, mechanical properties and corrosion behavior of an AA2219 friction stir weldments, *J. Alloys Compd.*, 2010, vol. 492, nos. 1–2, pp. 631–637.
9. Biju, S. Nair, Phanikumar, G., Prasad Rao, K., and Sinha, P.P., Improvement of mechanical properties of gas tungsten arc and electron beam welded AA2219 (Al–6 wt % Cu) alloy, *Sci. Technol. Weld. Join.*, 2007, vol. 12, no. 7, pp. 579–585.
10. Ji-kun Ding, Dong-po Wang, Ying Wang, and Hui Du, Effect of post weld heat treatment on properties of variable polarity TG welded AA2219 aluminum alloy joints, *Trans. Nonfer. Met. Soc. China*, 2014, vol. 24, pp. 1307–1316.
11. Bondarev, A.A., Electron beam welding of an Al–Cu–Mn alloy, *Avtosvarka*, 1974, vol. 2, no. 1, pp. 23–26.
12. Ma, T., Softening behaviour of Al–Zn–Mg alloys due to welding, *Mater. Sci. Eng. A*, 1999, vol. 266, no. 1, pp. 198–204.
13. Rao, S.R., Madhusudhana Reddy, G., Srinivasa Rao, K., Kamaraj,M., and Prasad Rao, K., Reasons for superior

mechanical and corrosion properties of 2219 aluminium alloy electron beam welds, *Mater. Charact.*, 2005, vol. 55, nos. 4–5, pp. 345–354.

14. Malarvizhi, S. and Balasubramanian, V., Influences of welding processes and post weld aging treatment on mechanical and metallurgical properties of AA2219 aluminium alloy joints, *Weld. World*, 2012, vol. 56, no. 18, pp. 105–119.
15. Gao, M., Feng, C.R., and Wei, R.P., An analytical electron microscopy study of constituent particles in commercial 7075-T6 and 2024-T3 alloys, *Metal. Mater. Trans. A*, 1998, vol. 29, no. 2, pp. 1145–1151.
16. Garland, J.G., Weld pool solidification control, *Brit. Weld. J.*, 1974, vol. 22, pp. 121–127.
17. Karunakaran, N. and Balasubramanian, V., Effect of pulsed current on temperature distribution, weld bead profiles and characteristics of gas tungsten arc welded aluminium alloy joints, *Trans. Nonfer. Met. Soc. China*, 2011, vol. 21, pp. 278–286.
18. Urena, A., Escalera, M. D., and Gil, L., Influence of interface reactions on fracture mechanisms in TIG arc-welded aluminium matrix composites, *Compos. Sci. Technol.*, 2000, vol. 60, no. 4, pp. 613–622.
19. Kou, S. and Le Y., Dendrite morphology in aluminium alloy welds, Metal. Trans., 1983, vol. 14 A, no. 2, pp. 2243–2249.
20. Malarvizhi, S., Raghukandan, K., and Viswanathan, N., Effect of post weld heat treatment on fatigue behaviour of electron beam welded AA2219 aluminium alloy, *Mater. Des.*, 2008, vol. 29, nos. 3–4, pp. 1562–1567.
21. Dieter, G.E., *Mechanical Metallurgy*, New York: McGraw Hill, 1988.
22. *Standard Test Methods for Tension Testing of Metallic Materials*, ASTM E8/ E8M-11, ASTM International.
23. Ber, L.B., Accelerated artificial ageing regimes of commercial aluminum alloys. I. Al–Cu–Mg alloys, *Mater. Sci. Eng. A*, 2000, vol. 280, pp. 83–90.